Video Article

Assessment of Right Ventricular Structure and Function in Mouse Model of Pulmonary Artery Constriction by Transthoracic Echocardiography

Hui-Wen Cheng*[1,2], Sudeshna Fisch*[1], Susan Cheng[1], Michael Bauer[1], Soeun Ngoy[1], Yiling Qiu[1], Jian Guan[1], Shikha Mishra[1], Christopher Mbah[1], Ronglih Liao[1]

[1]Cardiac Muscle Research Labratory, Cardiovascular Division, Brigham and Women's Hospital, Harvard Medical School

[2]Cardiovascular Department, Chang Gung Memorial Hospital

*These authors contributed equally

Correspondence to: Ronglih Liao at rliao@rics.bwh.harvard.edu

URL: http://www.jove.com/video/51041
DOI: doi:10.3791/51041

Keywords: Medicine, Issue 84, Trans-thoracic echocardiography (TTE), right ventricle (RV), pulmonary artery constriction (PAC), peak velocity, right ventricular systolic pressure (RVSP)

Date Published: 2/3/2014

Citation: Cheng, H.W., Fisch, S., Cheng, S., Bauer, M., Ngoy, S., Qiu, Y., Guan, J., Mishra, S., Mbah, C., Liao, R. Assessment of Right Ventricular Structure and Function in Mouse Model of Pulmonary Artery Constriction by Transthoracic Echocardiography. *J. Vis. Exp.* (84), e51041, doi:10.3791/51041 (2014).

Abstract

Emerging clinical data support the notion that RV dysfunction is critical to the pathogenesis of cardiovascular disease and heart failure[1-3]. Moreover, the RV is significantly affected in pulmonary diseases such as pulmonary artery hypertension (PAH). In addition, the RV is remarkably sensitive to cardiac pathologies, including left ventricular (LV) dysfunction, valvular disease or RV infarction[4]. To understand the role of RV in the pathogenesis of cardiac diseases, a reliable and noninvasive method to access the RV structurally and functionally is essential.

A noninvasive trans-thoracic echocardiography (TTE) based methodology was established and validated for monitoring dynamic changes in RV structure and function in adult mice. To impose RV stress, we employed a surgical model of pulmonary artery constriction (PAC) and measured the RV response over a 7-day period using a high-frequency ultrasound microimaging system. Sham operated mice were used as controls. Images were acquired in lightly anesthetized mice at baseline (before surgery), day 0 (immediately post-surgery), day 3, and day 7 (post-surgery). Data was analyzed offline using software.

Several acoustic windows (B, M, and Color Doppler modes), which can be consistently obtained in mice, allowed for reliable and reproducible measurement of RV structure (including RV wall thickness, end-diastolic and end-systolic dimensions), and function (fractional area change, fractional shortening, PA peak velocity, and peak pressure gradient) in normal mice and following PAC.

Using this method, the pressure-gradient resulting from PAC was accurately measured in real-time using Color Doppler mode and was comparable to direct pressure measurements performed with a Millar high-fidelity microtip catheter. Taken together, these data demonstrate that RV measurements obtained from various complimentary views using echocardiography are reliable, reproducible and can provide insights regarding RV structure and function. This method will enable a better understanding of the role of RV cardiac dysfunction.

Video Link

The video component of this article can be found at http://www.jove.com/video/51041/

Introduction

Historically, prognostic assessment of heart failure has focused on the LV, which is easy to image via echocardiography. Numerous studies on LV structure and function using echocardiography have led to the establishment of normal values for LV structure and function[1,5,6]. Measurements of LV size and systolic function obtained from two-dimensional and Color Doppler images are of great importance as they allow visual delineation of compartments and geometry in great detail for the LV[7]. M-Mode is often used for measuring LV dimensions and fractional shortening (FS) in mice. Inter-observer and intra-observer variability are low for diameter measurements using this mode, but wall thickness measurements tend to be quite variable[7]. Pulsed Doppler with color (PW or Color Doppler) has been used to evaluate valvular regurgitation[8,9].

Similar to LV, the RV plays an important role and is a significant predictor of morbidity and mortality in patients afflicted with cardiopulmonary disease[1,7,10]. However, echocardiographic evaluation of RV is inherently challenging due to its complex shape[5,11] and its retrosternal position that blocks the ultrasound waves[8,9]. RV is a crescent shaped structure wrapping around the LV and has a complex anatomy with thin walls that are accustomed to low pressure and resistance to pulmonary vasculature[6]. To overcome elevated vascular resistance (PVR), the RV first increases in size and undergoes hypertrophies. In chronic diseases like pulmonary hypertension or pulmonary vascular disease, RV undergoes progressive dilatation, eventually resulting in the deterioration of systolic and diastolic function[4,5,10].

Echocardiography plays an important role in the screening and diagnosis of PAH despite some limitations present in its clinical diagnostic capability. The main advantage of TTE lies in that it is noninvasive and that it can be performed on lightly sedated, or even conscious animals[9]. TTE also provides a reasonable estimate of PA pressures, as well as an ongoing assessment of changes in RV structure and function[12,13]. Due to technical advances in TTE, which include the development of high-frequency mechanical probes, allowing axial resolution of approximately 50 µm at a depth of 5-12 mm, high frame rates (greater than 300 frame/sec), and high sampling rates, echocardiography is a choice tool for imaging the rapidly contracting small sized mouse heart[8,11].

Longitudinal monitoring of RV function using multiple views, including 2-dimensional (2D) short and long axis, M-mode and Doppler acoustic windows provide complementary information of RV anatomy and function. Collectively, this methodology permits complete longitudinal assessment of RV hemodynamics in physiology and pathological setting[4,7].

Herein, we provide a detailed step-by-step methodology of using noninvasive TTE to characterize RV anatomical and functional changes secondary to PAC in mice.

Protocol

Surgical Procedure

1. Obtain 8 week-old male C57BL/6 mice and acclimate for one week before any experimental procedures are performed.
2. Prior to imaging, pulmonary artery occlusion is performed as described previously[14] in accordance with AVMA guidelines and approved IACUC protocols.

Echocardiographic Images Acquisition and Measurements

All abbreviations used are summarized in **Table 1**.

1. Parasternal Long Axis (PLAX) M Mode View to Obtain RV Chamber Dimension, Fractional Shortening (FS), and RV Wall Thickness

1. Use B Mode setting to obtain a full LV parasternal long axis view. With the animal lying in a supine position on the platform (see Note 6.1. and 6.2.), position the 40 MHz ultrasound probe (MS550D) on the animal with about 30° angle counterclockwise to the left parasternal line with the notch pointing caudal direction (**Figure 1A**). Adjust the probe angle by tilting slightly along y-axis of the probe (**Figure 1D**) to obtain a full LV chamber view in the center of the screen.
2. Once the proper landmarks (RV, LV, MV, Ao, LA) as illustrated in **Figures 2A** and **2B** are clearly visualized, switch to M Mode. An indicator line will show up on the screen in the M Mode setting. The line should be positioned to go through the widest portion of RV chamber using Ao as landmark (**Figures 2A** and **B**).
3. In this view, the RV wall and IVS should be clearly visible. Please ensure that the focus depth lies in the center of RV chamber. Record the data with cine store for measurement RV chamber dimension, FS and RV wall thickness off line. Examples of M Mode images are shown in **Figures 2C** and **2D**. (See Note 6.3.)

2. Parasternal Short-axis View at Mid Papillary Level to Obtain Fractional Area Changes (FAC)

1. From the position described above (**Figure 1A**), switch to B Mode and turn the probe 90° clockwise to obtain the parasternal short-axis view (**Figure 1B**). Tip the probe slightly along the x-axis of the probe to prevent the obstructive view of the sternum.
2. Move slightly up and down along the y-axis of the probe to obtain the mid papillary level (See Note 6.4.)
3. In this view, the papillary muscles are typically located at the 2 and 5 o'clock position (**Figure 3**).

3. Parasternal Short-axis View at Aortic Valve Level (RV PSAX Aortic Level) to Obtain RV Wall Thickness and PA Peak Velocity

1. From the position described above (**Figure 1B**), move the probe at the y-axis toward cranium until the aortic valve cross section shows in the middle of the window.
2. Right ventricular outflow tract (RVOT) should be visible on the top as a crescent-shaped structure with tricuspid valve separating the RV from RA as illustrated in **Figures 4A** and **2B**. Record the data using cine store for the measurement of RV wall thickness off line. (See Note 6.5.)
3. Remain at the same position. (See Note 6.6.)
4. Switch to Color Doppler Mode and position the yellow PW- dashed line parallel to the direction of flow in the vessel. Note that blue and red colors indicate flow away from and toward the probe, respectively (**Figures 4C** and **4D**).
5. Place the PW cursor at the tip of the pulmonary valve leaflets. (See Note 6.7.) Record data using cine store. Measure PA peak velocity off line.

4. Modified Parasternal Long-axis View of RV and PA to Obtain PA Peak Velocity

1. Continue on B Mode setting, position the probe (MS550D or MS250) to right parasternal line (**Figure 1C**) and slowly title the probe about 30-45° angle on the y-axis of the probe (**Figure 1D**) toward the chest of the mice to clearly visualize the PA crossing over aorta as illustrated in **Figures 5A** and **5B**.
2. Switch to Color Doppler Mode and position the yellow PW- dashed line parallel to the direction of flow in the vessel (**Figures 5C** and **5D**). Place the PW cursor at the tip of the pulmonary valve leaflets. (See Note 6.6.) Record data using cine store and measure PA peak velocity off line.

5. Data Calculation and Analysis

1. RV wall thickness can be calculated from the B Mode data obtained from RV PSAX aortic level as described above (Protocol 3). Select the 2D area tracing tool to trace the area of the RV wall at diastole (as shown in pink area in **Figure 6**). Then, use the distance tracing tool to trace the inner and outer circumferences of the wall of RVOT (as shown in blue lines in **Figure 6**). Take the average of inner and outer circumferences. Using the equation $\mathrm{RVW} = \frac{\text{RV area}}{\text{length}}$, we calculate RV Wall (RVW) thickness. (See Note 6.8.)
2. For other standard parameters, please refer to the manuals from the respective manufactures to perform data analysis.

6. Notes

1. All images are collected using the Vevo 2100 system. Similar images may be obtained using ultrasound imaging systems from other manufacturers, and the relative pros and cons of various ultrasound instruments have been previously compared[8,12,15]. It is recommended that all images should be obtained and analyzed in a blinded fashion whenever possible.
2. The proper choice of anesthesia, such as a short duration of inhaled isoflurane (2-3% to induce, and 1.0% to maintain) is crucial in the maintenance of heart beat at normal physiological rates (above 500 beats/min), allowing us to detect reproducible and consistent basal and elevated pulmonary arterial systolic pressure in the study.
3. Make sure to collect the data at the highest possible frame rate possible (>200 frames/sec).
4. Look for the view with the largest chamber dimension.
5. Obstruction due to ribs and the sternum largely due to the RV's retrosternal position is the single biggest impediment to obtaining excellent images in this method of imaging the RV. By repositioning the animal or the probe, an operator can overcome the sternal block and obtain necessary views of the RV. This may take from 5-15 min, depending on the animal's physiology.
6. You may need to switch probe to MS250 since MS550D probe can be used in sham and mice before PAC and the 40 MHz probe is capable to record peak velocity of 300-1,500 m/sec, whereas MS250 is able to capture the park velocity up to 4,000 mm/sec.
7. It is acceptable to have a probe angle less than 20° for accurate measurement of PA peak velocity.
8. Consistent measurements of RV wall thickness and area/dimensions were made using multiple acoustic windows, in both the long- and short-axis. The choice of some of these windows will depend on the experience of the operator, and could account for variability that could be contributory to different statistical results.

Representative Results

In this study, baseline echocardiography was performed 48 hr prior to surgery. Mice were randomized into two groups. Mice received pulmonary artery occlusions (PAC) and sham operations (Sham). Echocardiography was performed at day 0, 3, and 7 following surgical procedure. The animals were euthanized immediately following the last echocardiography and hearts were harvested for histological assessment. Catheterization was conducted in subgroup (n=3 and 2 for day 0 and 7, respectively) of PAC mice to measure RVSP via pressure catheter.

All imaging data obtained was analyzed off line. Importantly, sonographers were blinded to the procedures that the animals underwent. The images presented in this study were taken by two independent imagers. The inter- and intra- observer variability was tested, and found to be less than 6 % and 11%, respectively. The measurements were obtained using all available acoustic windows- B Mode, M Mode and Color Doppler images taken together were used in assessment of RV structure and function. All measurements were averaged over 5 cardiac cycles. For each measurement, the mean value and standard deviation (SD) was obtained. Often similar measurements were performed from different imaging windows to obtain complementary information and multiple data-points for comparison of accuracy and reliability.

As shown in **Figures 7A** and **7B**, systolic function of RV can be measured in PLAX view as %FS or in mid papillary muscle view as %FAC, respectively. While the decrease in FAC was already significant at day 0, the decrease in FS was only significant at day 7 (n=6, $P<0.01$). One major caveat of this view is that because of the retrosternal position of RV and occasionally due to the obstruction posed by the ribs, much care should be taken to obtain the RV image to accurately demonstrate the maximum diameter of the right ventricle without foreshortening the image. Small variations in RV diameter can mask small but significant changes in function. In contrast, %FAC is markedly decreased following PAC, even at day 0 right after the PA occlusion (n=6, $P< 0.05$) and decreased progressively overtime (n=6, $P< 0.001$). Thus, %FAC should be used as a primary measure of RV function and %FS as a secondary measure. It is noteworthy that %FAC has been shown to be a reliable predictor of heart failure, sudden death, stroke and/or mortality[3,4,10,16].

The RV dilatation can be measured in the long- and short-axis as RV chamber dimension (RVIDd) and RV area in diastole (**Figures 7C** and **7D**). The reliability of echo derived RVIDd in small rodents is indeed not as dependable as those measures in humans. This represents an important caveat in measuring RVID in mice. In small animals, the RVID is more clearly visualized in the long axis view, rather than the apical four-chamber view, as is commonly done in humans. Importantly, though, the endocardial definition of the anterior wall is often suboptimal under

the long axis view and oblique imaging may underestimate size measures. We find that RV area measure in the mid papillary muscle view is a more reproducible and reliable surrogate for RV chamber dimension and RV dilatation in mice.

RV free wall thickness, as a marker of RV hypertrophy, can be determined accurately either using M Mode or the area-trace method (**Figures 7E** and **7F**). Similarly, the PA peak velocity can also be obtained with either at PLAX or SAX mode (**Figures 7G** and **7H**, respectively). Reliable measurements of PA peak velocity and thus, peak-pressure gradient within the PA can be obtained using Color Doppler in both short- and long- axis acoustic windows (**Figures 7G** and **7H**). It should be noted that these velocity measurements are angle dependent and hence, it is recommended to obtain velocities using multiple views and with similar sweep speed for all tracings (greater than 100 mm/sec).

Lastly, **Figure 8** shows that in noninvasive echocardiography is a viable alternative to the terminal right heart catheterization method used as the gold standard for RVSP measurement[9]. For the 5 animals, catheterization for comparison of RVSP measurement methods was performed, and calculations of pressure were highly comparable (Pearson correlation coefficient r=0.943, P>0.05). In echocardiography, the PA peak velocity is measured reliably, and it follows that the calculation from the PA peak velocity is also reproducible. Additionally, this method allows for serial measurement of the pulmonary pressure gradient over time.

In summary, the noninvasive echo-based imaging can be a useful tool to follow RV structural and functional remodeling longitudinally similar to what has been commonly used in LV.

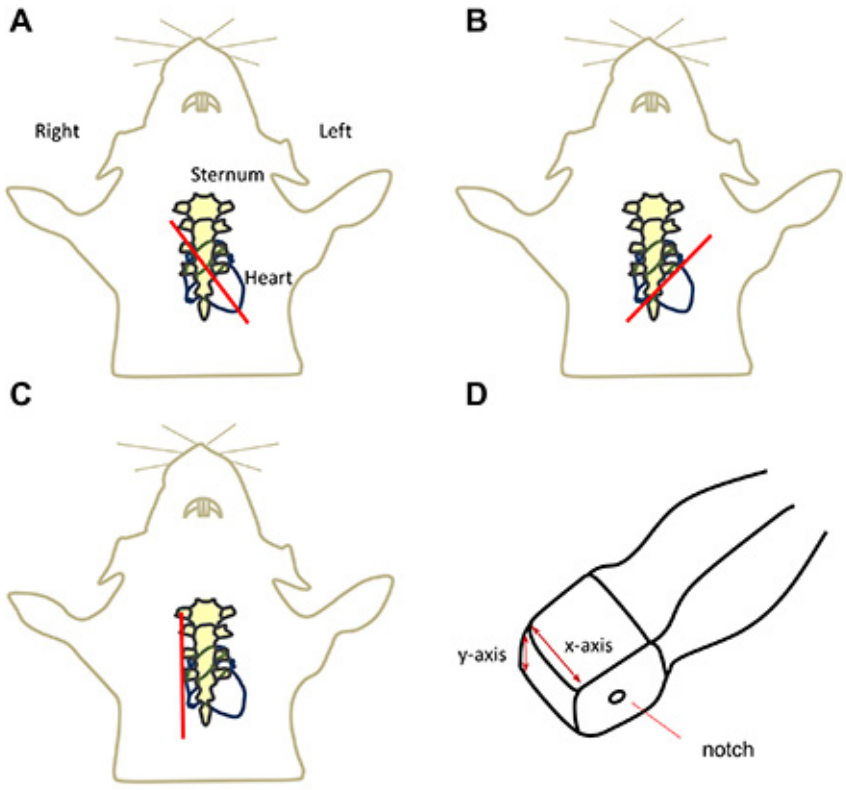

Figure 1. Graphical illustrations of the imaging probe position. Red line indicating the position of the probe for obtaining **A,** parasternal long axis **B,** parasternal short axis, **C,** modified parasternal long-axis view and **D,** the x-y direction of the probe. Click here to view larger image.

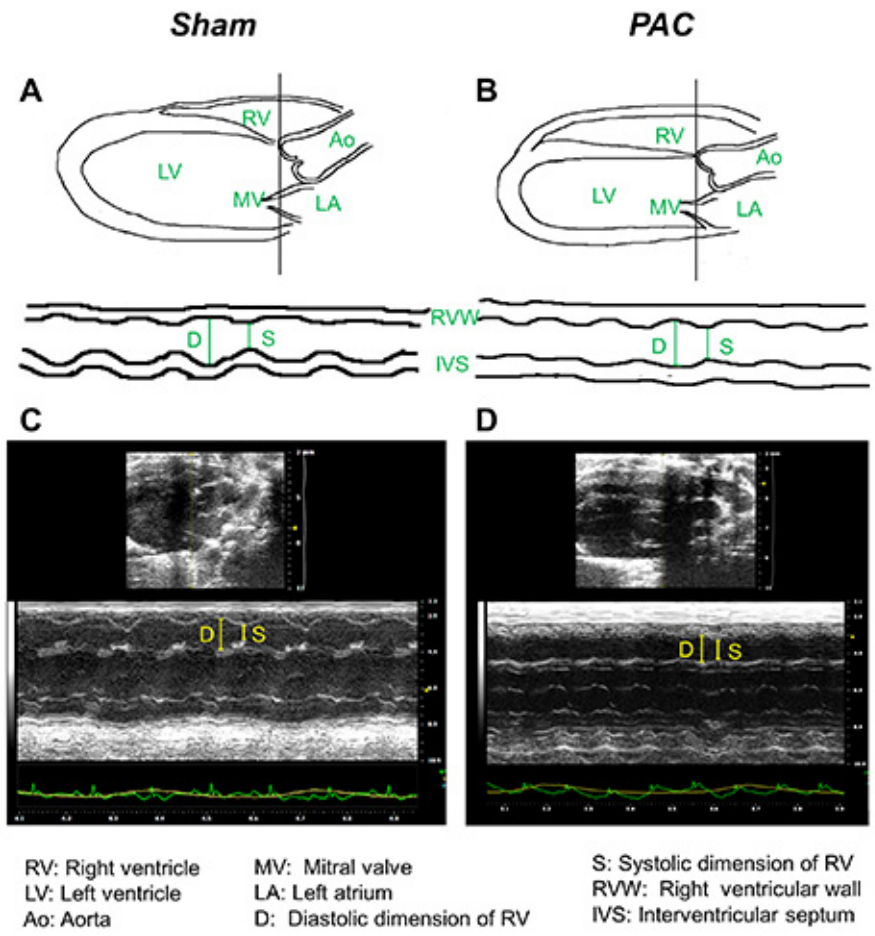

Figure 2. Parasternal long axis (PLAX) view. Graphical illustration and representative PLAX images from **A**, sham and **B**, PAC mouse heart. Key landmarks seen in the view areas follows. 1: Right ventricle (RV), 2: Left ventricle (LV), 3: Aorta (Ao), 4: Mitral valve (MV), 5: Left atrium (LA), 6: Diastolic dimension of right ventricle (D), 7: Systolic dimension of right ventricle (S), 8: Right ventricular wall (RVW), 9: Interventricular septum (IVS). Click here to view larger image.

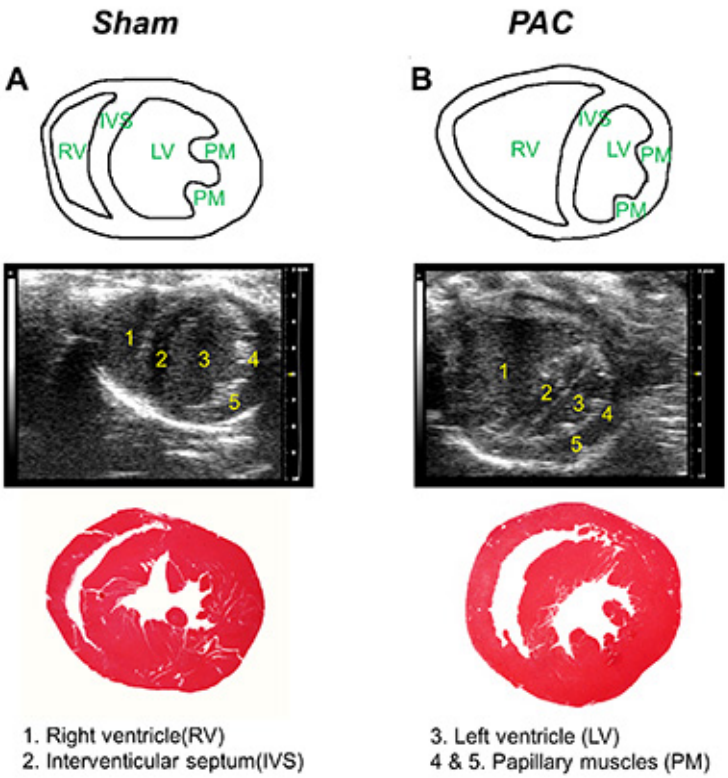

Figure 3. Parasternal short-axis view (PSAX) at mid-pap level of right ventricle (RV). Graphic illustration, representative image in PSAX at mid-papillary muscle level and H&E staining from **A**, sham and **B,** PAC mouse heart. Key landmarks seen in the view are as follows. 1: right ventricle (RV), 2: interventricular septum (IVS), 3: left ventricle (LV), and 4 & 5: papillary muscles. Click here to view larger image.

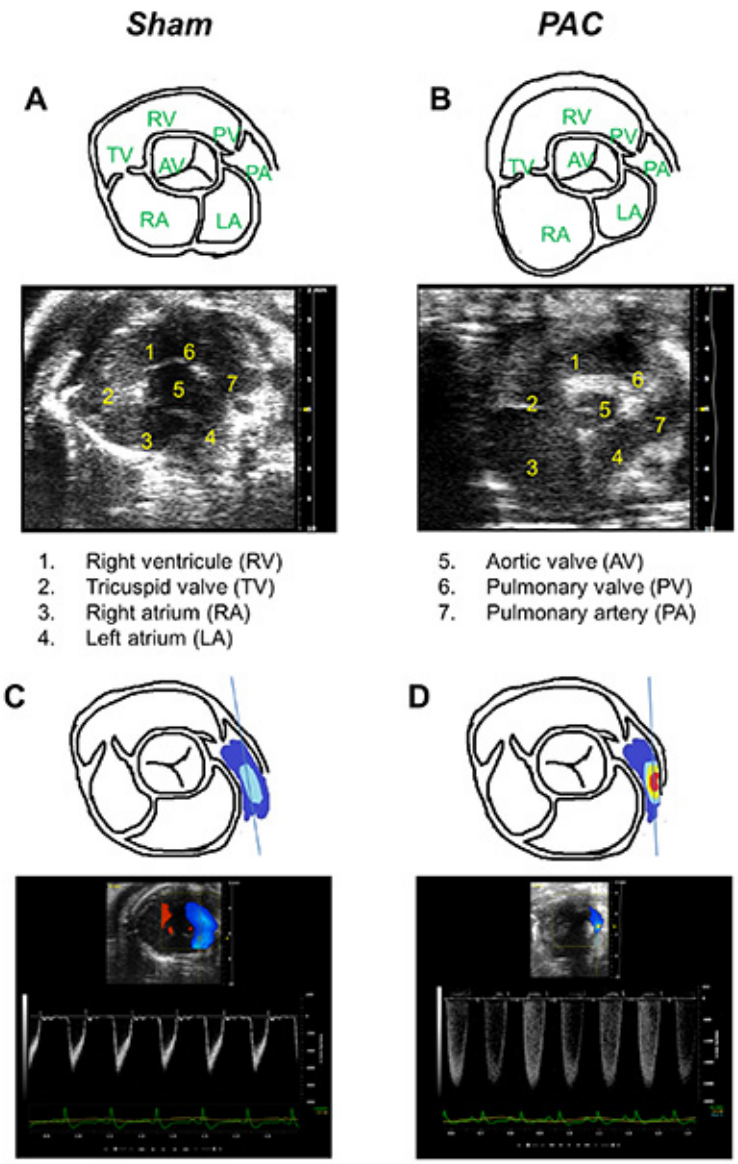

Figure 4. Parasternal short-axis view (PSAX) at aortic-level. Graphic illustration and representative B Mode images from **A**, sham and **B**, PAC mouse heart. Graphic illustration and Color Doppler images from **C**, sham and **D**, PAC mouse heart. Key landmarks seen in the view are as follows. 1: Right ventricular outflow tract (RVOT), 2: Tricuspid valve (TV), 3: Right atrium (RA), 4: Left atrium (LA), 5: Aortic valve (AV), 6: Pulmonary valve (PV), and 7: Pulmonary artery (PA). Click here to view larger image.

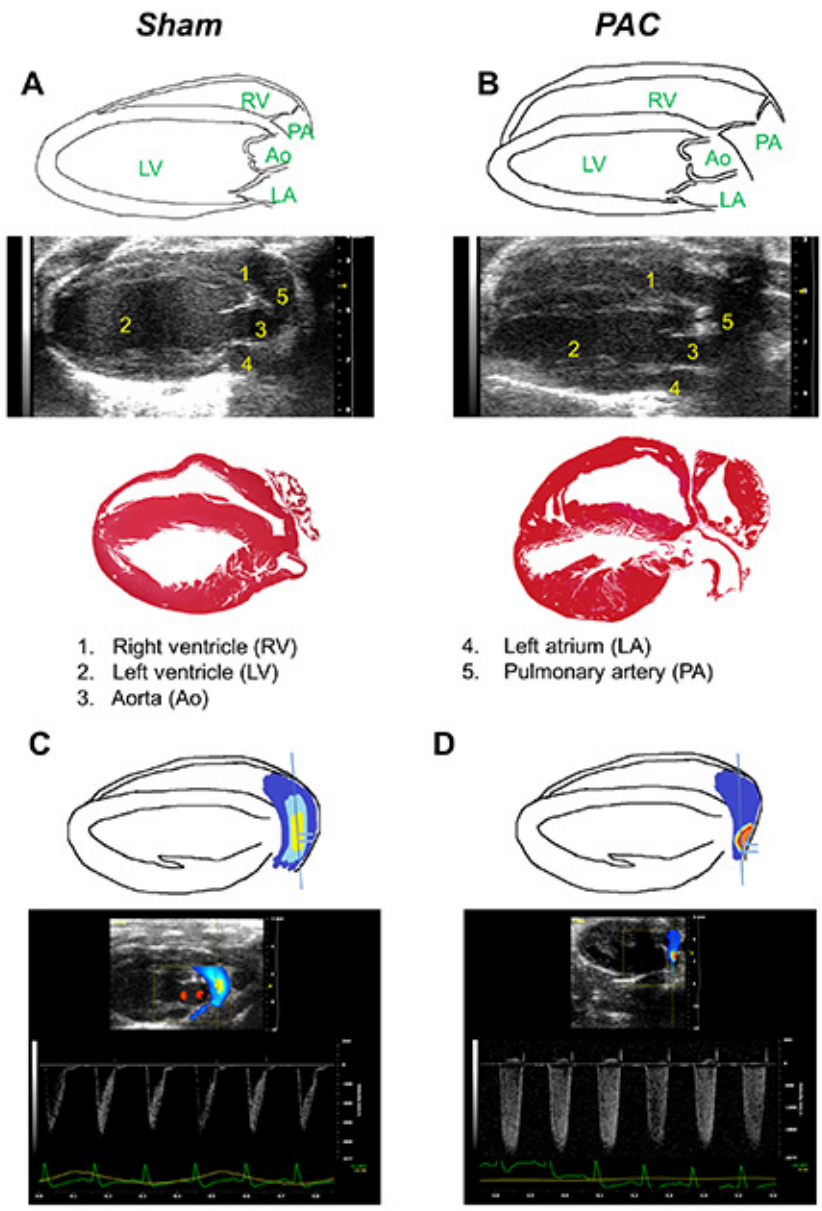

Figure 5. Modified parasternal long-axis (PLAX) view of right ventricle (RV) and pulmonary artery (PA). Graphical illustration, representative modified PLAX images, and H&E histology from **A**, sham and **B,** PAC mouse heart. Graphic illustration and Color Doppler images from **C**, sham and **D**, PAC mouse heart. Key landmarks seen in the view areas follows. 1: Right ventricle (RV), 2: Left ventricle (LV), 3: Aorta (Ao), 4: Left atrium (LA), and 5: Pulmonary artery (PA). Click here to view larger image.

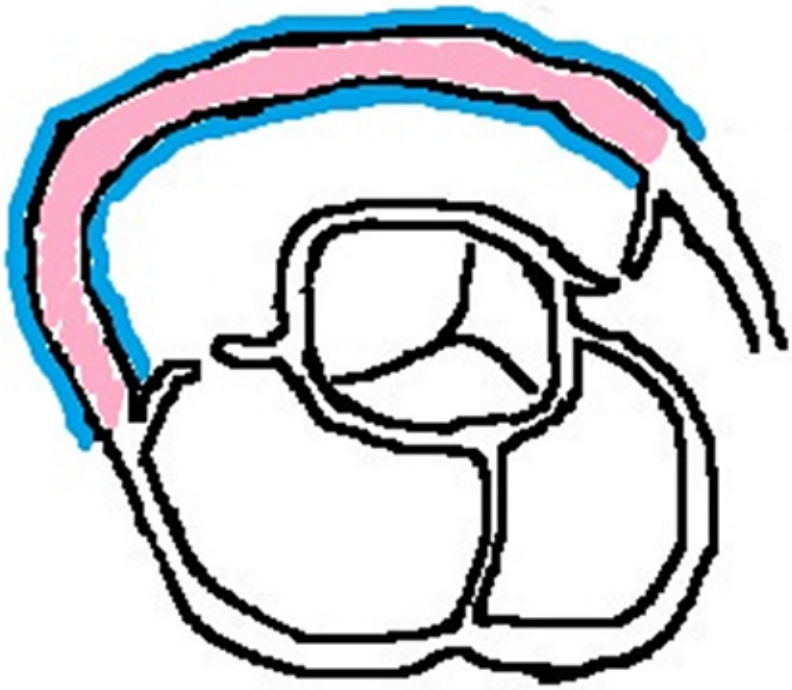

Figure 6. RV wall-thickness from Parasternal short-axis view (PSAX) at aortic level view. Graphical illustration of PSAX-image of heart section at aortic-level. Measurement of RV wall thickness can be derived from the area/length. Pink shade indicates area of RV free wall and blue line indicates inner and outer circumferences of RV.

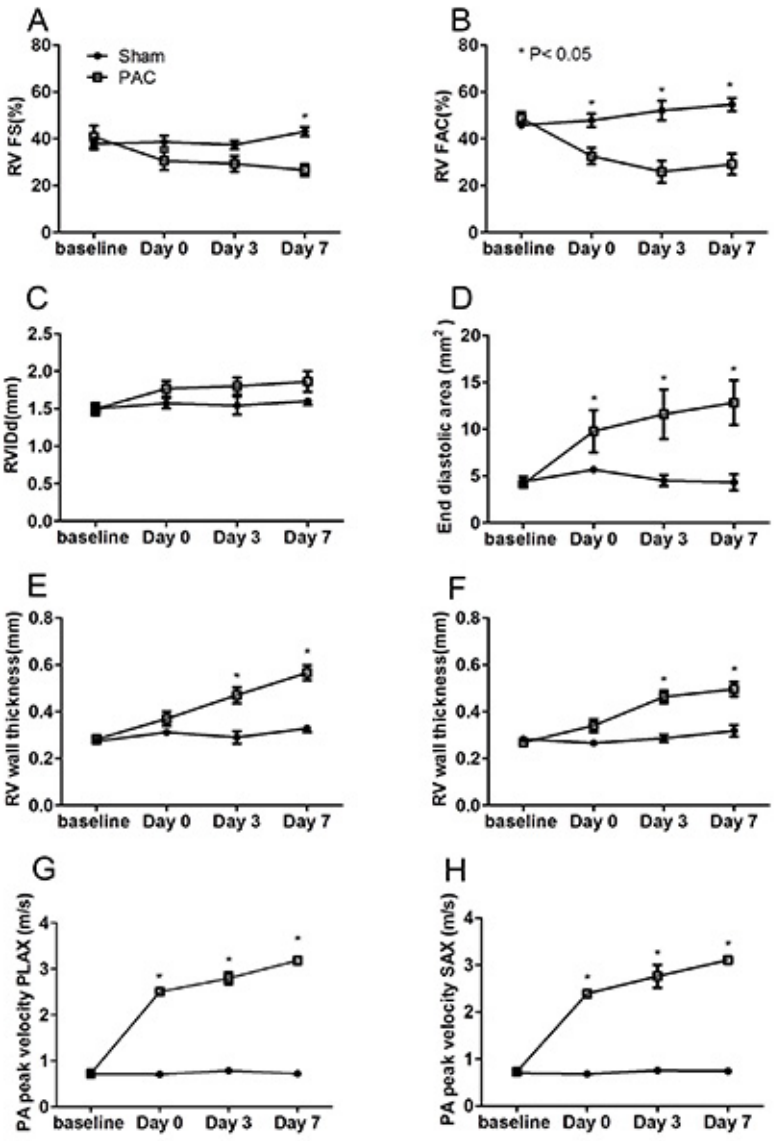

Figure 7. Structural and functional assessments of right ventricle (RV). **A**, Fractional shortening (FS) obtained using M mode at PLAX. **B,** Fractional area changes (FAC) obtained using PSAX at mid pap level. **C,** Right ventricular chamber dimension in diastole (RVIDd) obtained using M mode at PLAX. **D**, End diastolic right ventricular area obtained using PSAX at mid pap level. **E**, Right ventricular wall thickness at diastole obtained using M mode at PLAX and **F**, PSAX at aortic level. Pulmonary artery peak velocity obtained at **G**, modified PLAX at RV and PA view and **H**, PSAX at aortic level. Sham, n=6 and PAC, n=6, *, p<0.05. Click here to view larger image.

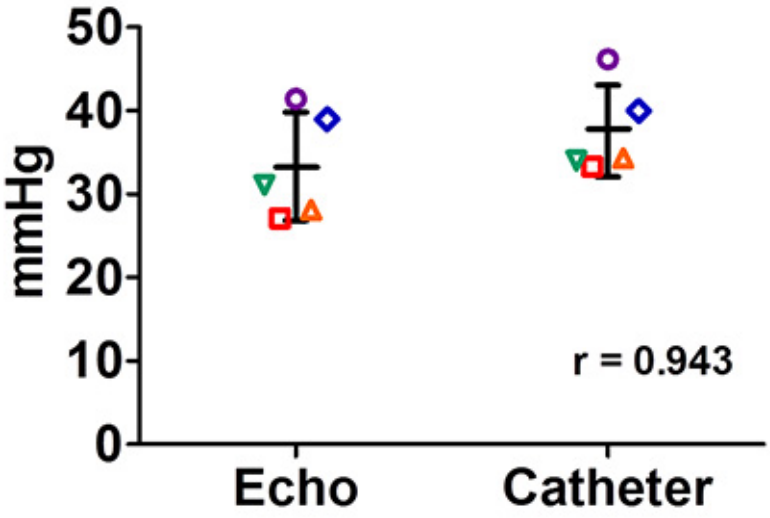

Figure 8. Correlation of pulmonary artery (PA) pressure measured using echocardiography (ECHO) and Millar microtip pressure catheter (Catheter). For echocardiography, peak-pressure gradient were calculated from PA peak velocities using modified Bernoulli's equation. The peak-pressure gradients (measured at site of constriction) were consistent with RVSP via catheterization with a correlation coefficient 0.943 (n=5).

Full name	Abbreviation
Left atrium	LA
Left ventricle	LV
Right atrium	RA
Right ventricle	RV
Aorta	Ao
Pulmonary artery	PA
Aortic valve	AV
Mitral valve	MV
Tricuspid valve	TV
Pulmonary valve	PV
Interventricular septum	IVS
Papillary muscle	PM
Fractional shortening	FS
Fractional area change	FAC
Parasternal long axis view	PLAX
Parasternal short axis view	PSAX
Transthoracic echocardiography	TTE
Pulmonary artery constriction	PAC
Right ventricular systolic pressure	RVSP
Pulmonary arterial hypertension	PAH
Right Ventricular outflow tract	RVOT
Right ventricular internal dimension in diastole	RVIDd

Table 1.

Discussion

We demonstrate that TTE provides a sensitive and reproducible methodology for routine assessment of RV structure and function in mice. Before the advent of TTE, studies of the RV largely focused on RVSP measurement via right heart catheterization, a terminal and invasive procedure[6,9,11,17].

Prior reports have described a variety of techniques for performing right heart measurements[3,4,11,17-19]. However, the majority of previous studies reported RV size and structural data in a predominantly qualitative rather than quantitative fashion[5]. A standardization of RV assessment is thus still in the beginning stages despite recent interest in RV function in the context of PAH and other models of diseases[9,19].

Taken together, these data provide evidence that noninvasive method of imaging can be a reliable and valuable tool for early evaluation of RV dysfunction. We established an imaging methodology to noninvasively visualize RV structural and functional changes in real time using a number of complementary imaging windows, and benchmarked our echo-based method of pressure-gradients against the conventional gold standard RVSP measurement by catheterization.

When imaged longitudinally, following an acute injury such as PAC, the RV undergoes rapid remodeling and the dynamic changes can be captured reproducibly through imaging. The image data coupled with the steps outlined in this methodology, along with further progress in technology such as 2D strain imaging, 3D echocardiography, and use of speckle-training[20] will improve a systematic echocardiographic evaluation of RV[12,15]. This could lead to increased therapeutic intervention in pathology of cardiopulmonary diseases by permitting earlier disease detection.

In summary, TTE can provide an essential first-step towards a comprehensive assessment of cardiac status and can serve as an effective discovery and assessment tool of physiological changes in structure and function. Because TTE is a noninvasive and widely accessible imaging modality, it offers the potential to aid investigations of cardiac diseases that require high-throughput and rapid data collection.

Disclosures

There is nothing to disclose.

Acknowledgements

We thank Fred Roberts and Chris White for exemplary technical support. We thank Brigham Women's Hospital Cardiovascular Physiology Core for providing with the instrumentation and the funds for this work. This work was supported in part by NHLBI grants HL093148, HL086967, and HL 088533(RL), K99HL107642 and the Ellison Foundation (SC).

References

1. Anavekar, N. S. *et al.* Usefulness of right ventricular fractional area change to predict death, heart failure, and stroke following myocardial infarction (from the VALIANT ECHO Study). *Am. J. Cardiol.* **101**, 607-612, doi:10.1016/j.amjcard.2007.09.115 (2008).
2. Berger, R. M., Cromme-Dijkhuis, A. H., Witsenburg, M. & Hess, J. Tricuspid valve regurgitation as a complication of pulmonary balloon valvuloplasty or transcatheter closure of patent ductus arteriosus in children < or = 4 years of age. *Am. J. Cardiol.* **72**, 976-977 (1993).
3. Marwick, T. H., Raman, S. V., Carrio, I. & Bax, J. J. Recent developments in heart failure imaging. *JACC Cardiovasc. Imaging.* **3**, 429-439, doi:10.1016/j.jcmg.2010.02.002 (2010).
4. Souders, C. A., Borg, T. K., Banerjee, I. & Baudino, T. A. Pressure overload induces early morphological changes in the heart. *Am. J. Pathol.* **181**, 1226-1235, doi:10.1016/j.ajpath.2012.06.015 (2012).
5. Karas, M. G. & Kizer, J. R. Echocardiographic assessment of the right ventricle and associated hemodynamics. *Prog. Cardiovasc. Dis.* **55**, 144-160, doi:10.1016/j.pcad.2012.07.011 (2012).
6. Lindqvist, P., Calcutteea, A. & Henein, M. Echocardiography in the assessment of right heart function. *Eur. J. Echocardiogr.* **9**, 225-234, doi:10.1016/j.euje.2007.04.002 (2008).
7. Rudski, L. G. *et al.* Guidelines for the echocardiographic assessment of the right heart in adults: a report from the American Society of Echocardiography endorsed by the European Association of Echocardiography, a registered branch of the European Society of Cardiology, and the Canadian Society of Echocardiography. *J. Am. Soc. Echocardiogr.* **23**, 685-713; quiz 786-688, doi:10.1016/j.echo.2010.05.010 (2010).
8. Scherrer-Crosbie, M. & Thibault, H. B. Echocardiography in translational research: of mice and men. *J. Am. Soc. Echocardiogr.* **21**, 1083-1092, doi:10.1016/j.echo.2008.07.001 (2008).
9. Thibault, H. B. *et al.* Noninvasive assessment of murine pulmonary arterial pressure: validation and application to models of pulmonary hypertension. *Circ. Cardiovasc. Imaging.* **3**, 157-163, doi:10.1161/CIRCIMAGING.109.887109 (2010).
10. Polak, J. F., Holman, B. L., Wynne, J. & Colucci, W. S. Right ventricular ejection fraction: an indicator of increased mortality in patients with congestive heart failure associated with coronary artery disease. *J. Am. Coll. Cardiol.* **2**, 217-224 (1983).
11. Tanaka, N. *et al.* Transthoracic echocardiography in models of cardiac disease in the mouse. *Circulation* **94**, 1109-1117 (1996).
12. Benza, R., Biederman, R., Murali, S. & Gupta, H. Role of cardiac magnetic resonance imaging in the management of patients with pulmonary arterial hypertension. *J. Am. Coll. Cardiol.* **52**, 1683-1692, doi:10.1016/j.jacc.2008.08.033 (2008).
13. Lang, R. M. *et al.* Recommendations for chamber quantification. *Eur. J. Echocardiogr.* **7**, 79-108, doi:10.1016/j.euje.2005.12.014 (2006).
14. Tarnavski, O., McMullen, J. R., Schinke, M., Nie, Q., Kong, S. & Izumo, S. Mouse cardiac surgery: comprehensive techniques for the generation of mouse models of human diseases and their application for genomic studies. *Physiol. Genomics.* **16**, 349-360, doi:10.1152/physiolgenomics.00041.2003 (2004).

15. Schulz-Menger. *et al.* Standardized image interpretation and post processing in cardiovascular magnetic resonance: Society for Cardiovascular Magnetic Resonance (SCMR) Board of Trustees Task Force on Standardized Post Processing. *J. Cardiovasc. Magn. Reson.* **15**, 35, doi:10.1186/1532-429X-15-35 (2013).
16. Williams, R. *et al.* Noninvasive ultrasonic measurement of regional and local pulse-wave velocity in mice. *Ultrasound Med. Biol.* **33**, 1368-1375, doi:10.1016/j.ultrasmedbio.2007.03.012 (2007).
17. Senechal, M. *et al.* A simple Doppler echocardiography method to evaluate pulmonary capillary wedge pressure in patients with atrial fibrillation. *Echocardiography.* **25**, 57-63, doi:10.1111/j.1540-8175.2007.00555.x (2008).
18. Frea, S. *et al.* Echocardiographic evaluation of right ventricular stroke work index in advanced heart failure: a new index? *J. Card. Fail.* **18**, 886-893, doi:10.1016/j.cardfail.2012.10.018 (2012).
19. Pokreisz, P. Pressure overload-induced right ventricular dysfunction and remodelling in experimental pulmonary hypertension: the right heart revisited. *Eur. Heart J. Suppl.* H75-H84, doi:10.1093/eurheartj/sum021 (2007).
20. Bauer, M. *et al.* Echocardiographic speckle-tracking based strain imaging for rapid cardiovascular phenotyping in mice. *Circ. Res.* **108**, 908-916, doi:10.1161/CIRCRESAHA.110.239574 (2011).

